The Plant Cell, Vol. 26: 1036–1052, March 2014, www.plantcell.org

Arabidopsis CAM7 and HY5 Physically Interact and Directly Bind to the *HY5* Promoter to Regulate Its Expression and Thereby Promote Photomorphogenesis[W]

Nazia Abbas,[a] Jay P. Maurya,[b] Dhirodatta Senapati,[b] Sreeramaiah N. Gangappa,[b] and Sudip Chattopadhyay[a,b,1]

[a] National Institute of Plant Genome Research, New Delhi 110067, India
[b] Department of Biotechnology, National Institute of Technology, Durgapur 713209, India

Arabidopsis thaliana **CALMODULIN7 (CAM7), a unique member of the calmodulin gene family, plays a crucial role as a transcriptional regulator in seedling development. The elongated HYPOCOTYL5 (HY5) bZIP protein, an integrator of multiple signaling pathways, also plays an important role in photomorphogenic growth and light-regulated gene expression. CAM7 acts synergistically with HY5 to promote photomorphogenesis at various wavelengths of light. Although the genetic relationships between *CAM7* and *HY5* in light-mediated seedling development have been demonstrated, the molecular connectivity between CAM7 and HY5 is unknown. Furthermore, whereas HY5-mediated gene regulation has been fairly well investigated, the transcriptional regulation of *HY5* is largely unknown. Here, we report that *HY5* expression is regulated by HY5 and CAM7 at various wavelengths of light and also at various stages of development. In vitro and in vivo DNA–protein interaction studies suggest that HY5 and CAM7 bind to closely located T/G- and E-box *cis*-acting elements present in the *HY5* promoter, respectively. Furthermore, CAM7 and HY5 physically interact and regulate the expression of *HY5* in a concerted manner. Taken together, these results demonstrate that CAM7 and HY5 directly interact with the *HY5* promoter to mediate the transcriptional activity of *HY5* during *Arabidopsis* seedling development.**

INTRODUCTION

Arabidopsis thaliana seedlings follow two contrasting developmental patterns in light and dark conditions. Skotomorphogenesis (or etiolation) in the dark is characterized by long hypocotyls, closed cotyledons protected by apical hooks, and the development of proplastids into etioplasts. By contrast, growth in the light results in photomorphogenesis (or deetiolation) characterized by short hypocotyls and open and expanded cotyledons with mature green chloroplasts (Nagatani et al., 1993; Whitelam et al., 1993; McNellis and Deng, 1995; Neff et al., 2000; Chen et al., 2004). Plants have adopted the ability to sense multiple parameters of ambient light signals, including light quantity (fluence), quality (wavelength), direction, and duration, through multiple photoreceptors. There are at least three distinct families of photoreceptors known: phytochromes, cryptochromes, and phototropins (Cashmore et al., 1999; Lin, 2002; Schepens et al., 2004; Jiao et al., 2007).

Calmodulin (CaM) is ubiquitous calcium sensor in eukaryotes. The EF-hands in CaM are organized into two distinct globular domains, each of which contains one pair of EF-hands (Zielinski, 1998; Reddy, 2001; Snedden and Fromm, 2001; Luan et al., 2002; Yang and Poovaiah, 2003; Hashimoto and Kudla, 2011). There are seven *Arabidopsis CAM* genes encoding proteins, which share 89% identity with vertebrate CaMs (McCormack et al., 2003). The *CAM* genes in *Arabidopsis* encode four protein isoforms: CAM1/CAM4, CAM2/CAM3/CAM5, CAM6, and CAM7. Whereas CAM1/CAM4 differs from CAM7 by four amino acids, CAM2/CAM3/CAM5 and CAM6 differ from CAM7 by a single amino acid substitution. Although four *Arabidopsis* CaM isoforms are highly similar, minor changes in CaMs contribute to target specificity selection (Bhattacharya et al., 2004; Grabarek, 2006; Kushwaha et al., 2008; Perochon et al., 2011).

Transcriptional regulatory networks have a key role in mediating the light signal through coordinated activation and repression of specific downstream genes. HYPOCOTYL5 (HY5) and CAM7/ZBF3 are the only known positive regulators of light signaling pathways that work under multiple wavelengths of light, including red light (RL), far-red light (FR), and blue light (BL) (Ang et al., 1998; Osterlund et al., 2000; Jiao et al., 2007; Kushwaha et al., 2008). It has been shown that CAM7 acts as a transcriptional regulator that directly interacts with promoters of several light-inducible genes (Kushwaha et al., 2008). The ectopic expression of CAM7 causes hyperphotomorphogenic growth under various light conditions. Whereas *cam7* mutants do not display altered photomorphogenic growth, *cam7 hy5* double mutants display a super-tall phenotype (Kushwaha et al., 2008). The mutational analysis of the EF-hand region of CAM7 revealed that the EF-hand plays an important role in determining target specificity. For example, it has been shown that Mg^{2+} can structurally bridge four EF-hand–containing human DREAM proteins to DNA; however, Ca^{2+}-induced dimerization of DREAM disrupts DREAM–DNA interactions (Ikura et al., 2002; Osawa et al., 2005).

[1] Address correspondence to sudipchatto@gmail.com.
The author responsible for distribution of materials integral to the findings presented in this article in accordance with the policy described in the Instructions for Authors (www.plantcell.org) is: Sudip Chattopadhyay (sudipchatto@gmail.com).
[W] Online version contains Web-only data.
www.plantcell.org/cgi/doi/10.1105/tpc.113.122515

The distinct morphological shift from skotomorphogenic to photomorphogenic growth involves a regulated change in the expression of about one-third of the genes in *Arabidopsis* (Ma et al., 2001; Tepperman et al., 2001). It has been reported that the massive change in gene expression is mediated by several transcriptional cascades (Tepperman et al., 2001). The transcriptional network plays a key role in mediating the light signal through the coordinated activation and repression of downstream genes (Mallappa et al., 2008; Singh et al., 2012). HY5 has been genetically defined as a positive regulator based on its partially etiolated phenotype of light-grown mutant seedlings (Koornneef et al., 1980; Ang and Deng, 1994; Oyama et al., 1997; Pepper and Chory, 1997). HY5 encodes a bZIP protein that can physically interact with COP1 and is degraded by COP1 ubiquitin ligase in the dark (Oyama et al., 1997; Ang et al., 1998; Osterlund et al., 2000). DNA–protein interaction studies have revealed that HY5 specifically interacts with the G-box and is required for the proper activation of the G-box–containing promoters in light (Ang et al., 1998; Chattopadhyay et al., 1998a; Yadav et al., 2002).

Extensive studies have been performed on HY5-mediated gene regulation and its involvement in multiple hormonal signaling pathways (Cluis et al., 2004; Sibout et al., 2006; Jiao et al., 2007; Vandenbussche et al., 2007; Alabadí et al., 2008; Chen et al., 2008; Kushwaha et al., 2008). Recent chromatin immunoprecipitation (ChIP)-on-chip studies have shown that HY5 binds to the regulatory regions of a large number of genes that have diverse functions in plant growth and development (Lee et al., 2007). It has been shown that HY5 acts in the feedback downregulation of FAR-RED ELONGATED HYPOCOTYL1 expression by phyA signaling upon FR exposure (Li et al., 2010). The binding of HY5 to the *LIGHT-REGULATED ZINC FINGER1* (*LZF1*) promoter in vivo suggests that HY5 is needed but not sufficient for the induction of *LZF1* expression (Chang et al., 2008). It has been shown that HY5 binds to the G-box present in close proximity to the CCA1 binding site in *Lhcb* (Andronis et al., 2008). Besides, HY5 along with the phytochrome-interacting factor PIF3 positively regulates the anthocyanin biosynthesis gene flavonone 3-hydroxylase (Shin et al., 2007). Taking into consideration the involvement of HY5 in various signaling and metabolic pathways, it is suggested that HY5 could act as a signal transducer that links various signaling pathways to coordinate growth and development (Jiao et al., 2007; Lee et al., 2007).

Although HY5-mediated gene expression has been extensively studied, the transcriptional regulation of *HY5* remains largely unknown. *HY5* has been shown to be expressed in various tissues, including roots, hypocotyls, cotyledons, leaves, stems, and flowers (Oyama et al., 1997). The accumulation of HY5 has been shown to be at its highest level at 3 d after germination, and the level steadily decreases afterward and is detectable up to at least 7 d. The level of accumulation of HY5 increases again during flowering time (Hardtke et al., 2000). In this study, we have investigated the biochemical interactions of CAM7 and HY5 proteins with the *HY5* promoter and between CAM7 and HY5 through in vitro and in vivo studies. We have further analyzed their in vivo functional interactions by examining the effects of *cam7* and *hy5* mutations on the activity of the *HY5* promoter in stable transgenic plants. Our data strongly support that CAM7 and HY5 physically interact, that both of these proteins bind to the *HY5* promoter, and, furthermore, that these interactions are critical for the optimal activation of the *HY5* promoter.

RESULTS

The T/G- and E-Boxes of the *HY5* Promoter Are Required for HY5 Interaction

Despite the fact that *HY5* is a major regulator of photomorphogenesis, the regulation of *HY5* expression is poorly understood. The in silico analysis of the upstream promoter sequence of *HY5* revealed that it contained a T/G-box and an E-box in close proximity and ~260 bp upstream to the transcriptional start site (Figure 1A). We performed electrophoretic mobility-shift assays to test whether the HY5 bZIP protein directly interacts with these *cis*-acting elements. For these experiments, we used a purified glutathione *S*-transferase (GST)-HY5 fusion protein and a 127-bp DNA fragment (−204 to −330 bp) containing the T/G-box and E-box in gel-shift assays (Figure 1A).

As shown in Figure 1B, GST-HY5 was able to bind to the 127-bp DNA fragment with high affinity, forming a DNA-protein complex (Figure 1B, lane 3). GST alone did not show any binding activity (Figure 1B, lane 2). Moreover, excess unlabeled 85-bp DNA fragment containing the T/G- and E-boxes was able to compete for the binding activity of GST-HY5 (Figure 1B, lanes 4 and 5). However, excess unlabeled 85-bp DNA fragments containing a mutated T/G-box and wild-type E-box (mT/G), mutated E-box and wild-type T/G-box (mE), or mutated T/G- and E-boxes (mT/G&E) were unable to compete for the binding activity of GST-HY5 (Figures 1A and 1B, lanes 6 to 11). These results indicate that the interaction of HY5 with the T/G- and E-boxes is specific. These results also suggest that both the T/G- and E-boxes are required for the interaction. To further test whether HY5 could bind to the T/G- or E-box alone, we performed gel-shift experiments using an 85-bp DNA fragment containing wild-type T/G- and E-boxes (Wt T/G&E), mutated T/G-box and wild-type E-box (mT/G), mutated E-box and wild-type T/G-box (mE), or mutated T/G- and E-boxes (mT/G&E). Although GST-HY5 could strongly bind to the wild-type T/G- and E-boxes containing the DNA fragment, it did not form any DNA-protein complex with other DNA fragments containing either wild-type T/G-box or wild-type E-box alone (Figure 1C). These results further demonstrate that HY5 requires both the T/G- and E-boxes for interaction with its own promoter.

To further substantiate the above results, we performed ChIP experiments. We used a HY5 overexpresser (HY5OE) transgenic line for this study (Lee et al., 2007). The HY5 protein was immunoprecipitated using anti-HY5 antibody, and the genomic DNA fragments that coimmunoprecipitated with HY5 were analyzed by quantitative real-time PCR. The amount of DNA fragment of the *HY5* promoter coimmunoprecipitated from wild-type and HY5OE transgenic seedlings was ~10-fold enriched as compared with the *hy5* mutant background or the *NIA2* promoter (AT1G37130), which is induced by light but does not

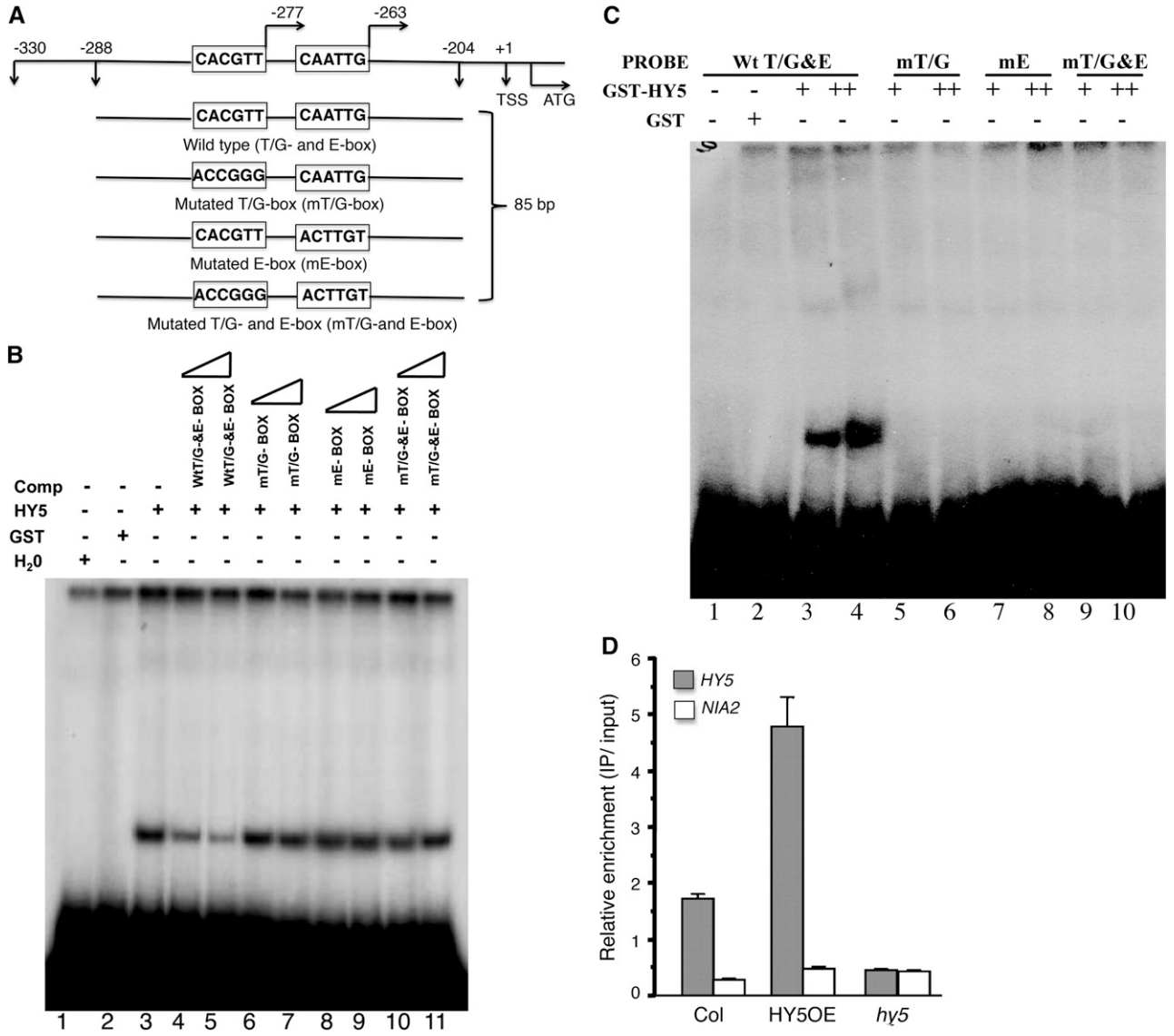

Figure 1. HY5 Directly Binds to the T/G- and E-Boxes of the *HY5* Promoter in Vitro.

(A) Diagrammatic representation of a 127-bp (−204 to −330 bp) *HY5* promoter fragment containing the T/G- and E-boxes used in the electrophoretic mobility-shift assay. The numbers indicate the distance from the transcriptional start site (TSS). The competition was performed by the 85-bp (−204 to −288 bp) wild type (Wt T/G&E), mutated T/G-box and wild-type E-box (mT/G), mutated E-box and wild-type T/G-box (mE), or mutated T/G- and E-box (mT/G&E), as shown. The wild-type and mutated versions (in red) of the T/G- and E-box sequences are given in the boxes.

(B) Gel-shift assays using GST-HY5 and the 127-bp T/G- and E-boxes containing the *HY5* promoter as probe. No protein was added in lane 1, and ~500 ng of GST protein was added in lane 2. In lanes 3 to 11, ~300 ng of GST-HY5 protein was added. Competition was performed with 50 (lanes 4, 6, 8, and 10) and 100 (lanes 5, 7, 9, and 11) molar excess of wild-type or mutated versions of the 85-bp DNA fragment of the *HY5* promoter, as shown by the triangles. The plus and minus signs indicate presence and absence, respectively.

(C) Gel-shift assays using GST-HY5 and 85-bp wild-type or various mutated versions of the T/G- and E-boxes (as shown in **[A]**) containing *HY5* promoter as probe. No protein was added in lane 1, and ~500 ng of GST protein was added in lane 2. In lanes 3, 5, 7, and 9, ~300 ng of GST-HY5 was added, and in lanes 4, 6, 8 and 10, ~600 ng was added.

(D) ChIP assays of the *HY5* promoter from Col-0, HY5OE, and *hy5* mutant seedlings using antibodies to HY5. The light-inducible *NIA2* promoter fragment that does not contain any T/G- or E-box was used as a control (Kushwaha et al., 2008). The results of quantitative real-time PCR are presented as the ratio of the amount of DNA immunoprecipitated from Col-0, HY5OE, or *hy5* mutants to input DNA from various backgrounds. The error bars indicate SD of three technical replicates. The experiment was repeated three times, and a representative result is shown.

contain any T/G- or E-box element (Figure 1D; Kushwaha et al., 2008). Taken together, these results demonstrate that HY5 binds to the *HY5* promoter in vivo.

HY5 Positively Regulates the Activity of Its Own Promoter

To examine whether the observed HY5 and T/G- and E-box interaction has a functional relevance in vivo, we asked whether the activities of the *HY5* promoter were affected in *hy5* mutants. Light responsiveness is usually conferred by promoter regions containing multiple light-responsive elements (LREs) (Tobin and Kehoe, 1994; Terzaghi and Cashmore, 1995). Several studies have indicated that a native minimal promoter that responds to light and developmental signals usually consists of at least one pair of LREs (Degenhardt and Tobin, 1996; Feldbrügge et al., 1997; Chattopadhyay et al., 1998b; Yadav et al., 2002). Therefore, it would be important to determine whether HY5 plays a role in the regulation of its own promoter containing the T/G- and E-box elements. To investigate this possibility, we constructed stable transgenic lines. A *ProHY5-GUS* construct was introduced into *Arabidopsis* plants (Columbia-0 [Col-0]) by stable transformation, and several homozygous transgenic lines were generated for the transgene (Supplemental Figure 1). One representative transgenic line containing the *ProHY5-GUS* transgene was used to introduce the transgene into the *hy5* null mutant (*hy5-215*) background through genetic crosses. Homozygous *hy5* mutant transgenic lines were then generated for further studies.

We monitored the activity of the *HY5* promoter as reflected by the β-glucuronidase (GUS) reporter enzymatic activity measurements. The activity of the *HY5* promoter in dark-grown seedlings was restricted to cotyledons in the wild-type background, whereas it was hardly visible in any tissue type of the *hy5* mutants (Figures 2A and 2B). Examination of the GUS staining pattern in white light (WL) revealed that the *ProHY5-GUS* transgene was expressed in cotyledons, hypocotyls, and roots of 5-d-old seedlings. Although a similar expression pattern of *ProHY5-GUS* was observed in *hy5* mutants, the level of expression was drastically reduced (Figure 2A). The GUS activity measurements revealed that the *HY5* promoter activity was ~17-fold less in *hy5* mutants than in the wild-type background in WL (Figure 2C). Taken together, these results indicate that HY5 is required for the optimal expression of *HY5* in WL. These results further suggest that HY5 is essential for the expression of *HY5* in dark-grown seedlings. A genomic fragment containing *HY5* and its upstream promoter sequence was introduced into the *hy5* mutants containing the *ProHY5-GUS* transgene for a complementation test. The transgenic seedlings were unable to display the reduced activity of the *HY5* promoter, suggesting that the observed reduction in *HY5* promoter activity in *hy5* mutants was caused by the loss of *HY5* function (Supplemental Figure 2A).

To determine the light-mediated induction kinetics of the *HY5* promoter in the wild type versus *hy5* mutants in WL, we transferred 4-d-old dark-grown seedlings to WL for various time periods and measured GUS activity. As shown in Figure 2D and Supplemental Figure 2B, whereas the *HY5* promoter was induced to ~2- to 3-fold in the wild type, there was little induction, if any, of the *HY5* promoter after 48 h of exposure to WL in the *hy5* mutant background. These results indicate that the inducibility of the *HY5* promoter was significantly compromised in *hy5* mutants.

HY5 Promotes the Activity of Its Own Promoter at Various Wavelengths of Light

Since HY5 works at various wavelengths of light, including RL, FR, and BL, we then tested whether the HY5-mediated activation of the *HY5* promoter was also present at various wavelengths of light, such as RL, FR, and BL. For these experiments, we used 5-d-old wild-type and *hy5* mutant transgenic seedlings grown in constant BL, RL, or FR. The *HY5* promoter conferred significantly decreased *GUS* expression in the cotyledons, hypocotyls, and roots in *hy5* seedlings compared with the wild-type background (Figure 2A). The quantification of GUS activity measurements revealed that the activity of the *HY5* promoter was ~14-fold reduced in *hy5* mutants as compared with the wild type in BL and RL (Figures 2E and 2F). The level of reduction of *HY5* promoter activity was found to be ~6-fold lower in *hy5* mutant as compared with wild-type seedlings in FR (Figure 2G). These results together imply a critical role for HY5 in the activation of the *HY5* promoter at various wavelengths of light.

HY5 Plays an Important Role in the Regulation of Its Own Expression in Both Photosynthetic and Nonphotosynthetic Tissues of Adult Plants

The morphological defects of *hy5* mutants are strong in the hypocotyls, stems, and roots and less prominent in the cotyledons and leaves. Earlier studies have shown that HY5 regulates the light-regulated gene expression in various tissues of the plant (Oyama et al., 1997; Ang et al., 1998; Chattopadhyay et al., 1998a). Therefore, we wanted to determine the autoregulatory role of HY5 in various organs in early adult and flowering plants. We analyzed the effect of the *HY5* mutation on the expression of the *HY5* promoter in various organs by staining for GUS activity in both 15-d-old young adult plants and 30-d-old flowering plants grown under 16-h-light/8-h-dark cycles.

In 15-d-old dark-grown plants, the *HY5* promoter displayed significantly decreased *GUS* expression in the leaves of *hy5* as compared with the wild type (Figures 3A and 3B). No *GUS* expression was detected in stems or roots of either wild-type or *hy5* mutant plants in darkness (Figure 3B). In WL, the *HY5* promoter conferred significantly reduced *GUS* expression in the leaves, stems, and roots of *hy5* mutant plants compared with those of the wild type (Figures 3C to 3E). The effect was more pronounced in roots as compared with stems or leaves (Figures 3C to 3E and 3J). Whereas an ~5-fold reduction in *HY5* promoter activity was noticed in roots, a 1.5- to 2-fold reduction was observed in stems and leaves of *hy5* mutants as compared with the wild-type background (Figure 3J).

In 30-d-old flowering plants, the *HY5* promoter was strongly active in the adult leaves and flowers (Figures 3F and 3I). The quantification of GUS activities revealed that the *hy5* mutants

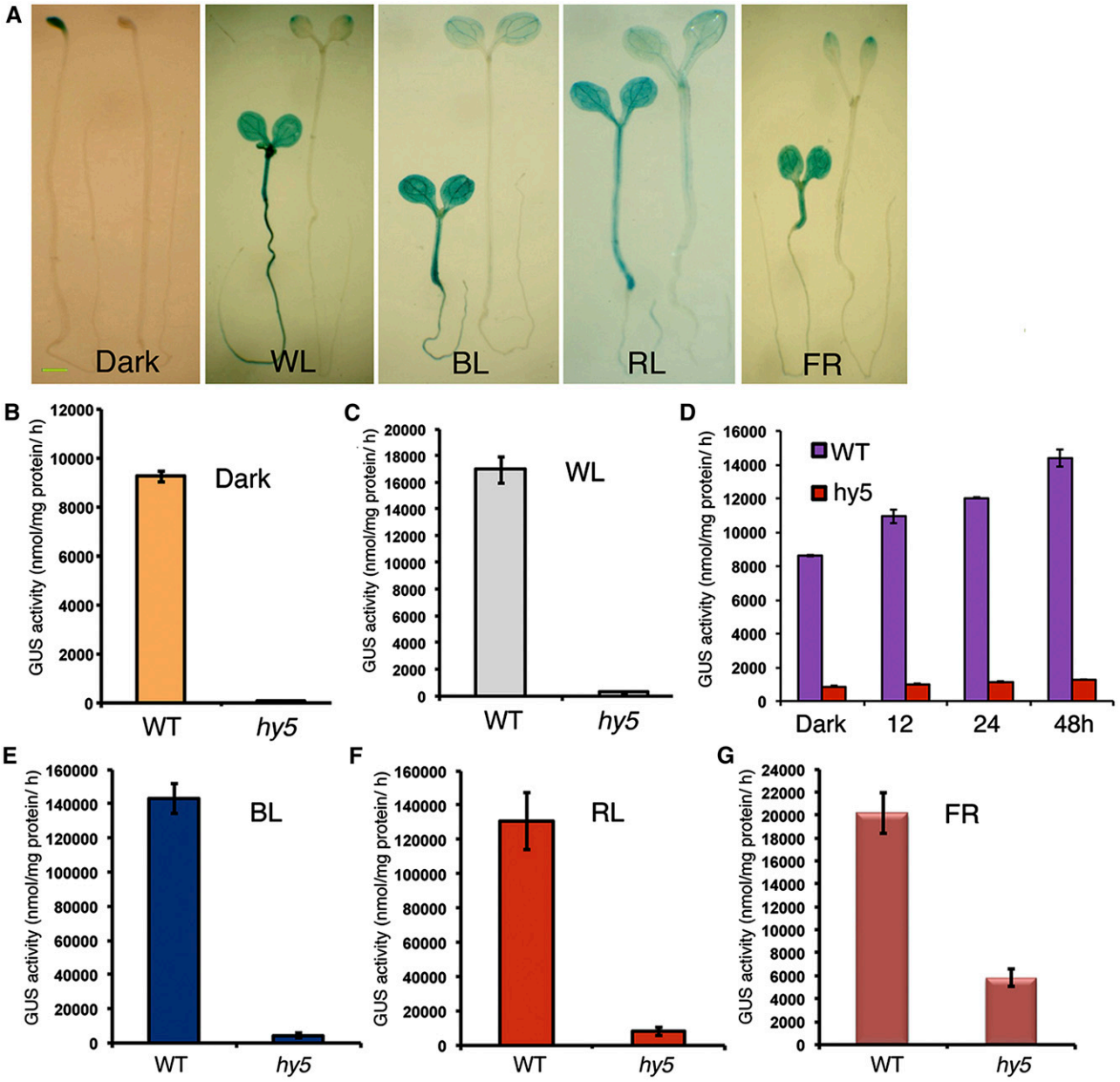

Figure 2. Effect of the *hy5* Mutation on the Wavelength-Specific Activation of the *HY5* Promoter.

In each panel of **(A)**, wild-type seedlings are shown on the left and *hy5* mutant seedlings are shown on the right. The quantitative GUS activities in **(B)** to **(G)** are averages of four technical repeats in one representative experiment (out of three), and the error bars indicate SD.

(A) Five-day-old seedlings carrying the *ProHY5-GUS* transgene were grown in constant darkness (dark), WL (80 μmol m^{-2} s^{-1}), BL (30 μmol m^{-2} s^{-1}), RL (40 μmol m^{-2} s^{-1}), or FR (30 μmol m^{-2} s^{-1}). The promoter activity in wild-type and *hy5-215* mutant backgrounds was estimated by quantitative GUS activity staining for the same length of time. Bar = 1 mm.

(B) and **(C)** GUS activity of 5-d-old constant dark–grown **(B)** or constant WL–grown **(C)** seedlings.

(D) GUS activity of 4-d-old dark-grown seedlings transferred to WL for 12, 24, and 48 h.

(E) to **(G)** GUS activity of 5-d-old BL-grown **(E)**, RL-grown **(F)**, and FR-grown **(G)** seedlings. The wild type and *cam7-1* and *hy5-215* mutants used are in the Col-0 background.

displayed significantly weaker activity than the wild type, with ~3-fold and ~5-fold reductions in leaves and flowers, respectively (Figure 3K). The *ProHY5-GUS* expression was found to be weak in stems and roots, and the activity was further decreased to ~1.5- to 2-fold in the *hy5* mutant background (Figures 3G, 3H, and 3K). In summary, these results strongly

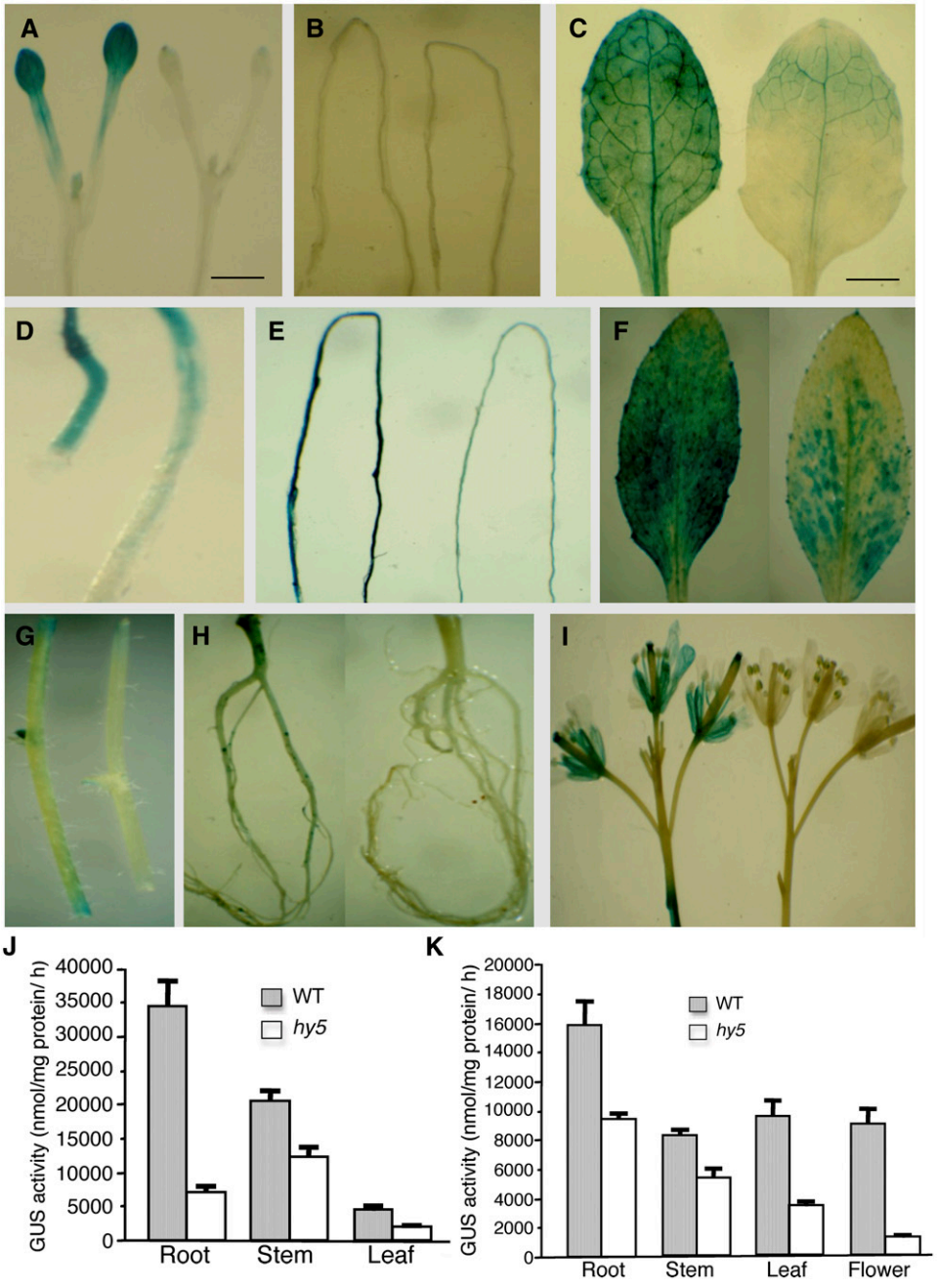

Figure 3. Effect of the *hy5* Mutation on the Tissue-Specific Expression of the *ProHY5-GUS* Transgene.

In each panel, wild-type seedlings are shown on the left and *hy5-215* mutant seedlings are shown on the right.
(A) and **(B)** Leaves **(A)** and roots **(B)** of 15-d-old dark-grown plants carrying the *ProHY5-GUS* transgene.
(C) to **(E)** Leaves **(C)**, stems **(D)**, and roots **(E)** of 15-d-old WL-grown (16-h-light/8-h-dark cycle) plants carrying the *ProHY5-GUS* transgene.
(F) to **(I)** Leaves **(F)**, stems **(G)**, roots **(H)**, and flowers **(I)** of 30-d-old WL-grown (16-h-light/8-h-dark cycle) plants carrying the *ProHY5-GUS* transgene.
(J) and **(K)** Quantification of GUS activities in leaves, stems, roots, and flowers. Promoter activities were monitored by measuring the GUS activities of wild-type and *hy5* mutant seedlings carrying the *ProHY5-GUS* transgene. The quantitative GUS activities are averages of four independent repeats in one representative experiment (out of four), and the error bars indicate SD. Comparison of GUS activities in roots, stems, and leaves of 15-d-old light-grown (16-h-light/8-h-dark cycle) plants of the wild type versus *hy5* mutants is shown in **(J)**, and comparison of GUS activities in roots, stems, leaves, and flowers of 30-d-old light-grown (16-h-light/8-h-dark cycle) plants of the wild type versus *hy5* mutants is shown in **(K)**.

demonstrate that the mutation in *HY5* caused reduced transcriptional activities of the *HY5* promoter as compared with the wild-type level, and this reduction was observed in all organs in which the promoter was found to be active.

CAM7 Directly Binds to the *HY5* Promoter

Since ZBF3/CAM7 specifically binds to the Z/G-box of light-regulated promoters and genetically interacts with HY5 to promote photomorphogenic growth and light-regulated gene expression (Kushwaha et al., 2008), we wanted to determine whether CAM7 also interacts with the *HY5* promoter containing the T/G- and E-box elements. We performed gel-shift assays using a purified GST-CAM7 fusion protein and a 127-bp DNA fragment (−204 to −330 bp) containing the T/G- and E-boxes (Figure 1A).

GST-CAM7 was able to interact with the 127-bp DNA fragment containing the T/G- and E-boxes with high affinity to form a DNA-protein complex (Figure 4A, lane 3). However, GST alone did not show any binding activity (Figure 4A, lane 2). The excess unlabeled 85-bp DNA fragment containing the T/G- and E-boxes was able to compete for the binding activity of GST-CAM7 (Figure 4A, lanes 4 and 5). However, excess unlabeled 85-bp DNA fragment of the *HY5* promoter containing mutated T/G-box and wild-type E-box (mT/G-box), mutated E-box and wild-type T/G-box (mE-box), or mutated T/G- and E-boxes (mT/G&E-box) were not able to compete for the binding activity of CAM7 (Figure 4A, lanes 6 to 11). Taken together, these results suggest that CAM7 interacts with the *HY5* promoter and that both T/G- and E-boxes are required for the DNA–protein interaction.

To investigate whether CAM7 could bind to the T/G- or E-box alone, we performed gel-shift experiments using 85-bp DNA fragments containing wild-type T/G- and E-boxes, mT/G-box, mE-box, or mT/G&E-box. Although CAM7 could strongly bind to the wild-type T/G- and E-box–containing DNA fragment, it did not form any DNA-protein complex with other DNA fragments containing either wild-type T/G- or E-box alone (Figure 4B). These results further demonstrate that CAM7 requires both the T/G- and E-boxes to interact with the *HY5* promoter.

To further substantiate the above results, we performed gel-shift experiments using a mutated version of CAM7, CAM7-M2, where four Asp residues were substituted by Ala in the EF-hands (Kushwaha et al., 2008). In this experiment, ~250 ng, 500 ng, and 1 μg of GST-CAM7-M2 and 250 and 500 ng of GST-CAM7 were added to a radioactively labeled 127-bp *HY5* promoter fragment. Whereas no DNA-protein complex was detected for CAM7-M2 and the *HY5* promoter (Figure 4C, lanes 5 to 7), a strong band of the DNA-protein complex of CAM7 and the *HY5* promoter was detected (Figure 4C, lanes 3 and 4). Taken together, these results suggest that four Asp residues in CAM7 are crucial for CAM7 binding to the *HY5* promoter.

We then performed a ChIP experiment to determine whether CAM7 interacts with the *HY5* promoter in vivo. For this experiment, *Arabidopsis* transgenic lines overexpressing CAM7 or CAM3 (as a control) fused to three copies of the cMyc epitope at the N-terminal end were used (Kushwaha et al., 2008; Supplemental Figure 3). The CAM7-cMyc and CAM3-cMyc overexpresser transgenic lines (CAM7OE and CAM3OE) were individually immunoprecipitated by antibody to cMyc protein. The genomic DNA fragments that coimmunoprecipitated with CAM7-cMyc and CAM3-cMyc were examined by quantitative real-time PCR. The analyses of these data revealed that the amount of DNA fragment of the *HY5* promoter coimmunoprecipitated from the CAM7-cMyc transgenic background was ~8-fold higher than that precipitated from nontransgenic seedlings. Furthermore, the enrichment of the *HY5* promoter in the CAM7-cMyc background was found to be ~8-fold higher than CAM3-cMyc and the *NIA2* promoter, as a control (Figure 4D). These results provide evidence that CAM7 directly interacts with the *HY5* promoter in vivo.

CAM7 Positively Regulates the Activity of the *HY5* Promoter

To determine the functional relevance of the observed CAM7 and *HY5* promoter interaction, we asked whether the activities of the *HY5* promoter were affected in the *cam7* mutants. To investigate that, the *ProHY5-GUS* transgene from the wild-type background was introduced into the *cam7* or CAM7OE background through genetic crosses (Kushwaha et al., 2008). The homozygous *cam7* mutant or CAM7OE transgenic lines were then generated for further studies.

The activity of the *HY5* promoter in 5-d-old dark-grown seedlings was mostly confined to cotyledons in the wild-type background. Although significantly reduced, the promoter activity remained restricted to cotyledons in the *cam7* mutant background (Figure 5A). On the other hand, the activity of the *HY5* promoter was detected both in the cotyledon and hypocotyl of the CAM7OE transgenic seedlings in darkness (Figure 5A). Quantification of the GUS activity revealed that whereas an ~2.5-fold increase was observed in CAM7OE transgenic lines, an ~2-fold reduction was observed in *cam7* mutants as compared with the wild-type background (Figure 5F). Examination of the GUS staining pattern in WL revealed that the *ProHY5-GUS* transgene was expressed in the cotyledons and hypocotyls of 5-d-old seedlings. Although similar expression patterns of *ProHY5-GUS* were observed in *cam7* mutants, the GUS stain was also detected in the roots of CAM7OE transgenic lines (Figure 5B). The GUS activity measurements revealed that the *HY5* promoter activity was ~2-fold reduced or increased in *cam7* and CAM7OE transgenic seedlings, respectively, compared with the wild-type background in WL (Figure 5F). Taken together, these results indicate that CAM7 is required for the optimal expression of *HY5* in dark- and WL-grown seedlings. These results further suggest that the ubiquitous expression of *CAM7* (in the CAM7OE line) could cause ectopic expression of *HY5* in roots in dark- and WL-grown seedlings.

Similar to HY5, CAM7 also functions at various wavelengths of light, including RL, FR, and BL. Therefore, we examined whether the CAM7-mediated activation of the *HY5* promoter was also present at various wavelengths of light. The *HY5* promoter conferred significantly altered *GUS* expression in the cotyledons, hypocotyls, and roots in *cam7* or CAM7OE lines

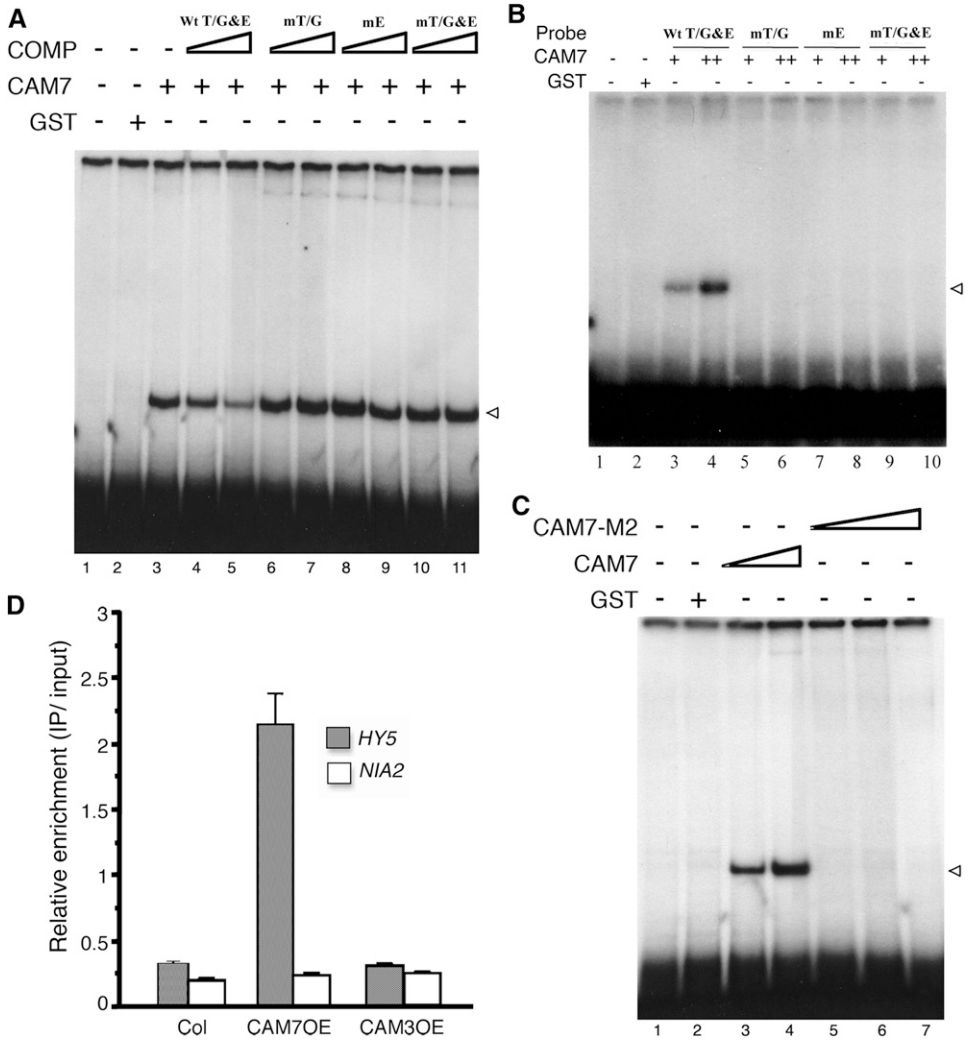

Figure 4. CAM7 Directly Binds to the T/G- and E-Boxes of the *HY5* Promoter in Vitro.

(A) Gel-shift assays using GST-HY5 and the 127-bp T/G- and E-boxes containing the *HY5* promoter as probe. No protein was added in lane 1, and ~500 ng of GST was added in lane 2. In lanes 3 to 11, ~300 ng of GST-CAM7 was added. The competition was performed using the 85-bp (−204 to −288 bp) wild type (Wt T/G&E), mutated T/G-box and wild-type E-box (mT/G), mutated E-box and wild-type T/G-box (mE), or mutated T/G- and E-boxes (mT/G&E), as shown in Figure 1A. Competition was performed with 50 (lanes 4, 6, 8, and 10) and 100 (lanes 5, 7, 9, and 11) molar excess of wild-type or mutated versions of an 85-bp DNA fragment of the *HY5* promoter, as shown by the triangles. The plus and minus signs indicate presence and absence, respectively. The arrowhead indicates the DNA-protein complex.

(B) Gel-shift assays using GST-CAM7 and the 85-bp wild-type or various mutated versions of T/G- and E-boxes containing the *HY5* promoter as probe. No protein was added in lane 1, and ~500 ng of GST was added in lane 2. In lanes 3, 5, 7, and 9, ~300 ng of GST-CAM7 protein was added, and in lanes 4, 6, 8, and 10, ~600 ng was added. The arrowhead indicates the DNA-protein complex.

(C) Gel-shift assays using GST-CAM7 or GST-CAM7-M2 protein and the 127-bp wild-type *HY5* promoter as probe. No protein was added in lane 1, and ~500 ng of GST was added in lane 2. In lanes 3 and 4, ~250 and 500 ng of GST-CAM7 was added, respectively; in lanes 5, 6, and 7, ~250 ng, 500 ng, and 1 μg of GST-CAM7-M2 was added, respectively. The arrowhead indicates the DNA-protein complex.

(D) ChIP assays of the *HY5* promoter from wild-type (Col-0), CAM7OE, and CAM3OE transgenic seedlings using antibodies to cMyc. The light-inducible *NIA2* promoter fragment that does not contain any T/G- or E-box was used as a control (Kushwaha et al., 2008). The results of quantitative real-time PCR are presented as the ratio of the amount of DNA immunoprecipitated from Col-0, CAM7OE, or CAM3OE to input DNA from various backgrounds. The error bars indicate SD of three technical replicates. The experiment was repeated three times, and a representative result is shown.

compared with the wild type (Figures 5C to 5E). The quantification of GUS activity measurements revealed that the activity of the *HY5* promoter was ~2- to 4-fold reduced in *cam7* mutants and ~1.4- to 2-fold increased in CAM7OE lines as compared with the wild type at various wavelengths of light (Figure 5F). These results demonstrate a critical role for CAM7 in the activation of the *HY5* promoter at various wavelengths of light.

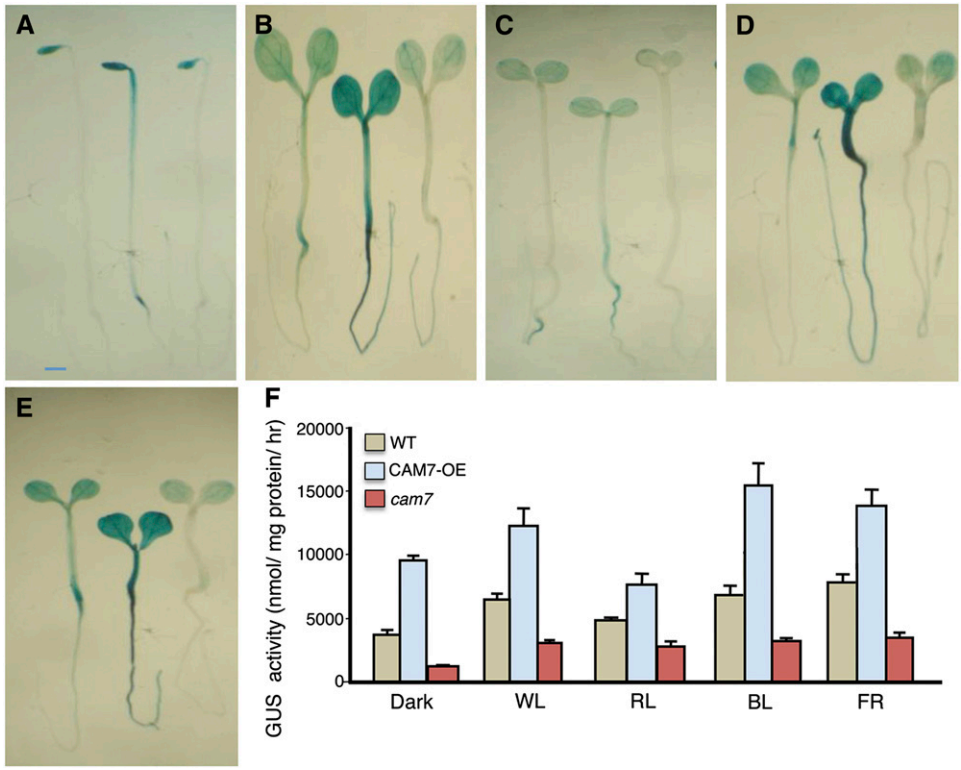

Figure 5. Effect of CAM7 on Wavelength-Specific Activation of the *HY5* Promoter.

In **(A)** to **(E)**, wild-type, CAM7OE, and *cam7* seedlings carrying the *ProHY5-GUS* transgene are shown from left to right, respectively. The quantitative GUS activities in **(F)** are averages of four independent repeats in one representative experiment (out of three), and the error bars indicate SD.
(A) to **(E)** Five-day-old seedlings carrying the *ProHY5-GUS* transgene were grown in constant darkness **(A)**, WL (30 μmol m^{-2} s^{-1} **[B]**), RL (30 μmol m^{-2} s^{-1} **[C]**), BL (30 μmol m^{-2} s^{-1} **[D]**), or FR (30 μmol m^{-2} s^{-1} **[E]**) for GUS activity staining. Bar = 1 mm.
(F) GUS activities of 5-d-old seedlings grown in constant darkness or various light conditions.

CAM7 Is a Positive Regulator of the *HY5* Promoter in Various Organs of Adult Plants

To determine the CAM7-mediated regulation of the *HY5* promoter in various organs in early adult and flowering plants, we analyzed the effect of the *CAM7* mutation and overexpression of CAM7 (CAM7OE) on the activity of the *HY5* promoter in various organs of both 15-d-old young adult plants and 30-d-old flowering plants grown under 16-h-light/8-h-dark cycles. In 15-d-old plants, the *HY5* promoter displayed decreased *GUS* expression in leaves, stems, and roots of *cam7* mutants as compared with those of the wild type (Figures 6A to 6C). The *GUS* expression was increased in all the organs tested in CAM7OE transgenic plants as compared with the wild-type background (Figures 6A to 6C). In 30-d-old flowering plants, the *HY5* promoter was active in adult leaves, stems, roots, and flowers (Figures 6D to 6G). The GUS activity measurements revealed that the *cam7* mutants displayed significantly weaker activity, with an ~2-fold reduction in leaves and flowers compared with the wild-type background (Figures 6F to 6H). The *ProHY5-GUS* expression was found to be weak in stems and roots, and the activity was further decreased to ~1.5-fold in the *cam7* mutant background (Figures 6D, 6E, and 6H). On the other hand, the activity of the *HY5* promoter was increased to ~2-fold in roots, stems, leaves, and flowers of CAM7OE transgenic lines compared with the wild-type background (Figures 6D to 6H). Taken together, these results demonstrate that the mutation in *CAM7* reduced the transcriptional activities of the *HY5* promoter as compared with the wild-type level, and this reduction was observed in all organs in which the promoter was found to be active. These results further demonstrate that higher levels of CAM7 can increase the activity of the *HY5* promoter.

CAM7 and HY5 Physically Interact with Each Other

Since CAM7 and HY5 genetically interact to promote photomorphogenesis (Kushwaha et al., 2008) and both of these proteins bind to the *HY5* promoter, we examined the possible physical interactions of CAM7 and HY5 through protein–protein interaction studies. First, we performed in vitro binding assays, in which we used poly-His or GST fusion proteins. For these experiments, GST or GST-HY5 protein was separately passed through columns containing empty nickel–nitrilotriacetic acid agarose (Ni-NTA) beads or beads attached to CAM7-His or COP1-His (as a positive control) proteins (Supplemental Figure 4; Ang et al., 1998). The anti-GST immunoblot showed that the amount of GST-HY5 retained by CAM7-His was comparable to

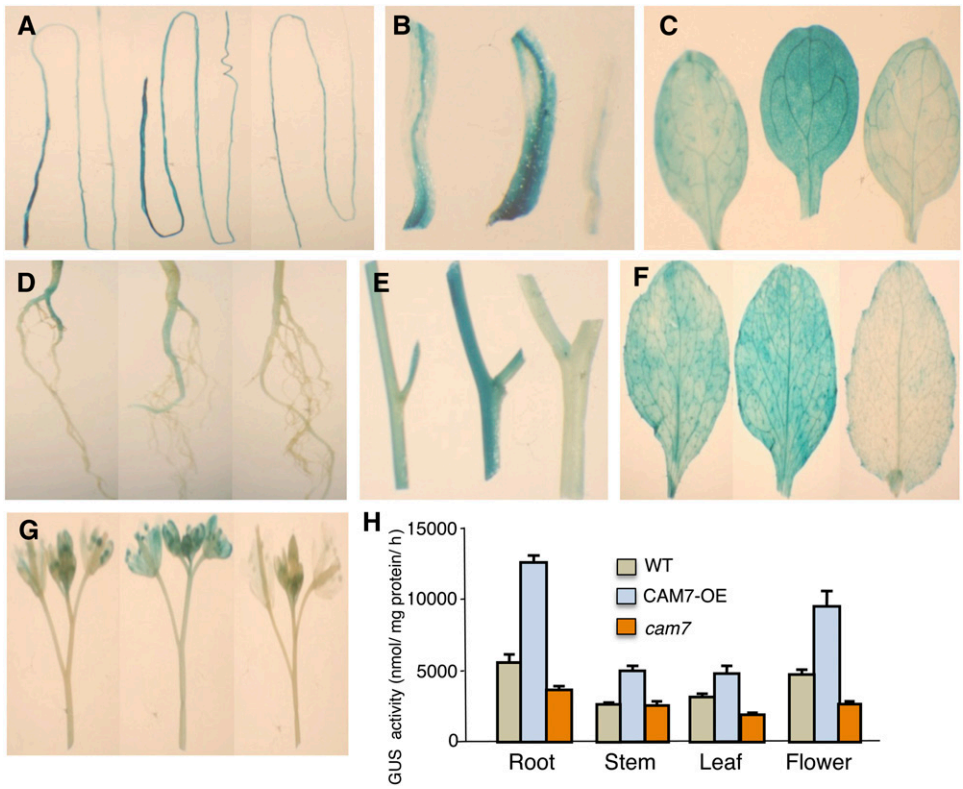

Figure 6. Effect of the *cam7* Mutation on the Tissue-Specific Expression of the *ProHY5-GUS* Transgene.

In **(A)** to **(G)**, wild-type, CAM7OE, and *cam7* seedlings carrying the *ProHY5-GUS* transgene are shown from left to right, respectively. The quantitative GUS activities in **(H)** are averages of four independent repeats in one representative experiment (out of three), and the error bars indicate SD.
(A) to **(C)** Roots **(A)**, stems **(B)**, and leaves **(C)** of 15-d-old WL-grown (16-h-light/8-h-dark cycle) plants carrying the *ProHY5-GUS* transgene.
(D) to **(G)** Roots **(D)**, stems **(E)**, leaves **(F)**, and flowers **(G)** of 30-d-old WL-grown (16-h-light/8-h-dark cycle) plants carrying the *ProHY5-GUS* transgene.
(H) Comparison of GUS activities in roots, stems, leaves, and flowers of 30-d-old WL-grown (16-h-light/8-h-dark cycle) plants.

COP1-His (Figure 7A). These results indicate that CAM7 physically interacts with HY5.

To further substantiate the above results, we performed in vitro pull-down assays using the total plant protein extracts. In this experiment, GST alone or GST-HY5 recombinant fusion protein was separately bound to glutathione Sepharose 4B beads and incubated with total protein extracts of the CAM7OE line. As shown in Figure 7B, while the protein extract was passed through the GST-HY5 column, CAM7 was retained in the column. The immunoblot analyses using anti-cMyc did not show any detectable band, while the protein extract was passed through the GST column. Taken together, these results strongly suggest that CAM7 physically interacts with HY5.

CAM7 Colocalizes and Physically Interacts with HY5 in Onion Cells

To determine the subcellular localization of interaction events of CAM7 and HY5, we prepared cyan fluorescent protein (CFP) or yellow fluorescent protein (YFP) fusion proteins of CAM7 and HY5. These constructs were cobombarded into the onion (*Allium cepa*) epidermal cells, and superimposition of the images of HY5-CFP with CAM7-YFP showed obvious color changes in fluorescence (Figure 7D) that were not apparent in images of the empty vectors (Figure 7C). Taken together, these results suggest that CAM7 colocalizes with HY5 in the nucleus of onion epidermal cells.

To confirm the in vivo physical interactions between CAM7 and HY5, a bimolecular fluorescence complementation (BiFC) experiment was performed. For this experiment, the full-length CAM7 coding sequence was fused to the N terminus of YFP in the pUC-SPYNE vector and the full-length HY5 coding sequence was fused to the C terminus of YFP in the pUC-SPYCE vector (Singh et al., 2012). Whereas empty vectors did not produce any YFP fluorescence (Figure 7E), the interaction of CAM7 and HY5 produced strong YFP fluorescence in the nucleus (Figure 7F). Taken together, these results demonstrate that CAM7 physically interacts with HY5 in vivo.

CAM7 and HY5 Together Bind to the *HY5* Promoter and Regulate Its Expression

Since CAM7 and HY5 physically interact with each other, and both these proteins bind to the *HY5* promoter, we asked whether CAM7 and HY5 together bind to the *HY5* promoter. To

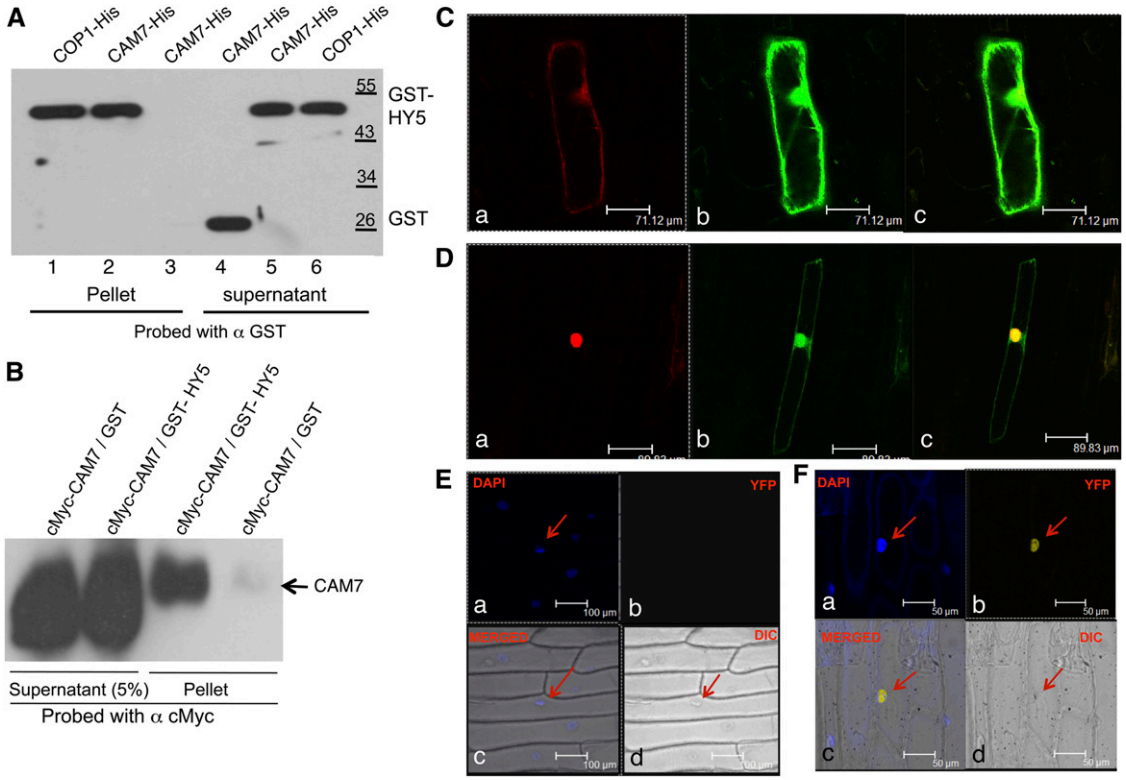

Figure 7. CAM7 Physically Interacts with HY5.

(A) In vitro binding of HY5 and CAM7. Approximately 2 μg of CAM7-6His or COP1-6His was individually bound to Ni-NTA beads. GST-HY5 or GST protein was added in equimolar ratio. Supernatant and pellet fractions were fractionated by SDS-PAGE, blotted, and probed with anti-GST antibodies. Lanes 1 and 6 show COP1-6His with GST-HY5 (positive control), lanes 2 and 5 show CAM7-6His with GST-HY5, and lanes 3 and 4 show CAM7-6His with GST.

(B) In vitro pull-down assays of cMyc-CAM7 and GST-HY5. GST and GST-HY5 proteins (1 μg each) were individually bound to GST beads. Approximately 1 mg of total protein extract from the CAM7-cMyc overexpression line was added and incubated at 4°C for 4 h. The supernatant and pellet were fractionated by SDS-PAGE, blotted, and probed with anti-cMyc antibodies.

(C) and **(D)** CAM7 colocalizes and interacts with HY5 in the nucleus of onion epidermal cells. In both panels, image **(a)** shows CFP channel fluorescence, changed to red color, **(b)** shows YFP channel fluorescence, changed to green color, and **(c)** shows merged images of **(a)** and **(b)**.

(E) and **(F)** Empty BiFC vectors **(E)** and CAM7-YFPN-ter and HY5-YFPC-ter constructs **(F)** were cotransformed into onion epidermal cells. In both panels, image **(a)** shows 4′,6-diamidino-2-phenylindole (DAPI) fluorescence for the confirmation of nuclei, **(b)** shows the YFP channel image produced by reconstruction of YFP, **(c)** shows merged images of **(a)** and **(b)**, and **(d)** shows the respective bright-field image (differential interference contrast [DIC]). Arrows indicate the positions of the nuclei.

examine this possibility, we performed ChIP assays using CAM7OE and CAM3OE transgenic lines. The transgenic lines were individually used to immunoprecipitate the possible *HY5 promoter*-CAM7-HY5 or *HY5 promoter*-CAM3-HY5 complex by using an antibody to cMyc. The immunoprecipitated complex was processed and subjected to immunoblot analyses using antibodies to HY5. Whereas no HY5 protein was detected in the CAM3OE transgenic line or wild-type background, a significant amount of HY5 was detected in the CAM7OE transgenic line (Figure 8A).

To further examine this phenomenon, we performed footprint experiments using a 127-bp *HY5* promoter fragment and HY5 and/or CAM7. The footprint analysis of the 127-bp promoter fragment showed that HY5 and CAM7 together protected a single 26-bp region around the T/G- and E-boxes from DNase I cleavage (Figure 8B; Supplemental Figure 5). Whereas most of the base pairs protected by HY5 were of the T/G-box, CAM7 protected mainly the E-box. Both proteins also protected the flanking base pairs and predominantly protected the base pairs between the T/G- and E-box region. These results demonstrate that HY5 and CAM7 specifically bind to the T/G-box and E-box, respectively, of the *HY5* promoter. Moreover, both proteins could bind simultaneously to the T/G- and E-box region of the *HY5* promoter.

To further examine whether binding of CAM7 to the *HY5* promoter is affected in the *hy5* mutant background in vivo, we performed ChIP assays using *hy5* CAM7OE transgenic lines (Kushwaha et al., 2008). As shown in Figure 8C, the amount of DNA fragment of the *HY5* promoter coimmunoprecipitated from the CAM7-cMyc transgenic background was slightly

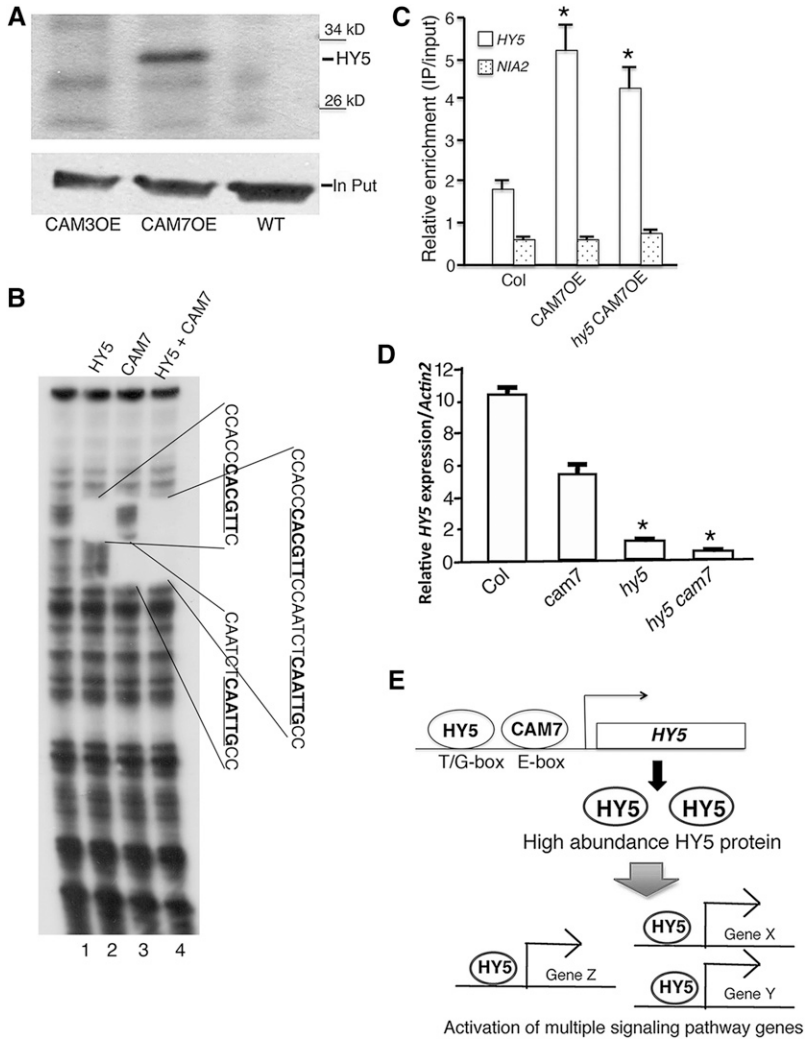

Figure 8. CAM7 and HY5 Together Bind to the *HY5* Promoter to Regulate *HY5* Expression.

(A) In vivo interactions between CAM7 and HY5 proteins in ChIP assays. The cross-linked complex of CAM7/HY5 with the *HY5* promoter was pulled down by antibodies to cMyc. The complex was reverse cross-linked and resolved by SDS-PAGE. Both the input and immunoprecipitates were probed with antibodies to HY5.

(B) DNase I footprinting analysis of the 127-bp *HY5* promoter fragment. Lane 1 shows the DNase I cleavage pattern with 20 μg of GST protein. Lanes 2 to 4 show the DNase I cleavage pattern with 20, 20, and 20 + 20 μg of the GST-HY5, GST-CAM7, and GST-HY5 + GST-CAM7 proteins, respectively. The protected DNA sequence containing the T/G- and E-box of the *HY5* promoter fragment is shown at right.

(C) ChIP assays of the *HY5* promoter from Col-0, CAM7OE, and *hy5* CAM7OE seedlings using antibodies to HY5. For experimental details, see the legend to Figure 1D. *P < 0.001 (Student's *t* test).

(D) Real-time PCR analysis of *HY5* transcript levels from 4-d-old WL-grown seedlings (30 μmol m^{-2} s^{-1}). *ACTIN2* was used as a control. Error bars represent SD. $n \geq 3$ independent experiments with similar results. *P < 0.01 (Student's *t* test).

(E) Working model of CAM7- and HY5-mediated regulation of *HY5*. HY5 and CAM7 bind to the *HY5* promoter to promote *HY5* expression. The accumulated HY5 protein then binds to a large number of promoters to activate multiple signaling and metabolic pathway genes.

reduced, if reduced at all, compared with that of the *HY5* promoter precipitated from *hy5* CAM7OE transgenic seedlings, suggesting that CAM7 is able to bind to the *HY5* promoter in the absence of HY5. To determine the level of expression of *HY5* in *hy5*, *cam7*, and *hy5 cam7* double mutant backgrounds, we performed quantitative real-time PCR analyses. Whereas the expression of *HY5* was ~2-fold reduced in *cam7* mutants compared with the wild-type control, an ~7-fold reduction in *hy5* expression was observed in *hy5* mutants. The level of expression of *HY5* was further reduced to ~12-fold in the *cam7 hy5* double mutant background (Figure 8D). Taken together, these results suggest that CAM7 and HY5 are required for and coordinately regulate the optimum expression of *HY5*.

DISCUSSION

This study demonstrates that CAM7 and HY5 interact with the *HY5* promoter and positively regulate the expression of *HY5* in a concerted manner at various stages of development. Characterization of the promoter elements involved in light regulation has been performed extensively (Gilmartin et al., 1990; Manzara et al., 1991; Anderson et al., 1994; Kehoe et al., 1994; Terzaghi and Cashmore, 1995). LREs, which commonly occur in light-regulated promoters, are essential for light-controlled transcriptional activity (Terzaghi and Cashmore, 1995; Arguello-Astorga and Herrera-Estrella, 1998). CAM7 interacts with the G- or Z-box of LREs and regulates the expression of light-inducible genes (Kushwaha et al., 2008). Although earlier studies had shown that HY5 could bind to the G-box LRE in the promoters of light-inducible genes, it was postulated that HY5 might also bind to other distinct promoter element(s), even with higher affinity (Chattopadhyay et al., 1998a). Recent studies have shown that HY5 is able to bind to the various imperfect G-boxes, such as the Z-box (ATACGTGT), C-box (GACGTC), hybrid C/G-box (GACGTG), and hybrid C/A-box (GATGCA) (Yadav et al., 2002, 2005; Mallappa et al., 2006; Shin et al., 2007; Song et al., 2008). It has also been found that HY5 is not able to bind to the single E-box element of the flavonone 3-hydroxylase gene promoter (Shin et al., 2007).

Recent studies have shown that the AT1- and I-box element in the *TOP2* promoter is recognized by a *trans*-acting factor for light-induced expression of *TOP2* (Hettiarachchi et al., 2003). The DNA–protein interaction studies performed in this study strongly demonstrate that HY5 and CAM7 bind to the T/G- and E-box elements, respectively, of the *HY5* promoter. The competition experiments in gel-shift assays further indicate that neither of the single *cis*-acting elements is sufficient for the binding activity of HY5 or CAM7. However, it is possible that both HY5 and CAM7 have more affinity to one of the *cis*-acting elements of the T/G- and E-boxes, where the nucleotides of the other *cis*-acting element or the nucleotides between these two elements strengthen the DNA-protein complex formed. Thus, although both elements are required for binding, which could be the requirement of the overall structure of the DNA spanning both elements, HY5 and CAM7 bind to the T/G-box and E-box, respectively. In other words, there is a difference between the sequence requirement for binding and the actual binding sites for these two proteins.

This possibility is further substantiated by the footprint and ChIP experiments (Figure 8). The footprint experiments of the *HY5* promoter with each of the proteins show that whereas HY5 binds to the T/G-box, CAM7 interacts with the E-box site, which is located next to the T/G-box (Figure 8B). The binding sites of HY5 and CAM7 encompassing the flanking nucleotides of the T/G- and E-boxes were observed in the footprint results. About 8- to 10-fold more enrichment of the *HY5* promoter was observed in HY5OE or CAM7OE transgenic lines as compared with mutants or transgenic lines used as a control in the ChIP assays (Figures 1 and 4). Detailed gel-shift and ChIP assays with the other regions of the 330-bp promoter fragment of *HY5* did not show any binding activity of HY5.

This study provides several lines of evidence for a direct role of HY5 and CAM7 in mediating *HY5* promoter activity in *Arabidopsis*. Whereas the strong activity of the *HY5* promoter was detected in light, the activity of the promoter was found to be weak in dark-grown seedlings. It is worth mentioning here that a lower percentage of 15-d-old early adult plants grew leaves in darkness (Rohde et al., 1999). Oyama et al. (1997) indicated that HY5 is ~15 to 20 times more abundant in seedlings grown in WL as compared with darkness, although the transcript levels of *HY5* show an ~2- to 3-fold difference between light- and dark-grown seedlings. In this study, the light-induced activation of the *HY5* promoter was found to be ~2-fold in the wild-type background and was compromised in *hy5* mutants (Figure 2D). The slight variation observed in the activity of the *HY5* promoter in wild-type seedlings is likely due to the various fluence rates used to grow the seedlings. Whereas the activity of the *HY5* promoter is restricted to cotyledons in the dark, the light-grown seedlings display the activity of the promoter in various tissue types. The reduced *HY5* promoter activity in darkness could be attributed to the lower level of HY5 accumulation. HY5 is degraded by COP1 ubiquitin ligase in the dark (Osterlund et al., 2000). Whereas the mutation in *CAM7* reduced the activity of the *HY5* promoter, the mutation in *HY5* completely abolished the *HY5* promoter activity in dark-grown seedlings. These results indicate that either there is little redundancy of HY5-like activities in darkness or HY5 activity is dominant in darkness as compared with other factors, such as CAM7.

Several lines of experimental results, including protein–protein interactions through BiFC experiments and in vitro pull-down assays using total plant protein extracts, demonstrate that CAM7 and HY5 physically interact with each other. One plausible mechanism of the physical interaction of CAM7 and HY5 may be that CAM7 acts as a modulator of HY5-mediated regulation of *HY5* expression and thereby regulates photomorphogenic growth. It has yet to be determined whether the CAM7-HY5-*HY5* promoter complex is present in seedlings grown at various wavelengths of light. CAM7 protein accumulates at higher levels in the dark and at lower fluences of WL, and these findings are in agreement with the role of CAM7 in photomorphogenesis (Kushwaha et al., 2008). On the other hand, HY5 accumulates at lower levels in darkness and at lower intensities of WL, and the level of HY5 protein increases with a higher intensity of light (Osterlund et al., 2000). It has been demonstrated that *cam7 hy5* double mutants display a super-tall phenotype, and overexpression of CAM7 in *hy5* mutants can partly suppress the etiolated phenotype of *hy5* mutants at lower intensities of light (Kushwaha et al., 2008). Therefore, one important aspect of the overlapping functions of HY5 and CAM7 may be that CAM7 and HY5 physically interact and regulate the expression of *HY5* during the transition from dark to light and at lower intensities of light.

The *hy5* or *cam7* mutation resulted in a significant reduction in the expression level of *ProHY5-GUS* in plants grown under WL; therefore, HY5 and CAM7 may work in parallel to regulate *HY5* expression (Figure 8E). The *hy5* mutation also severely compromised the light inducibility of the *HY5* promoter, as observed by the reduced response after transferring the dark-grown seedlings to WL. The negative effect of the null *hy5* and *cam7* mutations on *HY5* expression is partial in light, since residual activation is evident in various tissue types. Therefore, HY5 and

CAM7 are essential for the optimal level of expression of *HY5* in light-grown plants, although they do not seem to be the only regulatory proteins to promote the expression of the gene in light. The expression of *HY5* in the *cam7 hy5* double mutant also supports this notion (Figure 8D). HY5 is known to interact and form heterodimers with at least two other bZIP proteins, GBF1/ZBF2 and HYH, during *Arabidopsis* seedling development (Holm et al., 2002; Singh et al., 2012). Therefore, higher levels of HY5 might also interact or form heterodimers with other regulatory proteins in the regulation of *HY5* expression.

The activity of the *HY5* promoter in *hy5* and *cam7* mutants was compromised in both photosynthetic and nonphotosynthetic tissues of adult plants. The effect was more pronounced in *hy5* than in *cam7*. The higher level of CAM7 accumulation increased the activity of the *HY5* promoter under various light conditions and at various stages of development. A drastic reduction in GUS activity staining was observed in the roots of 15-d-old light-grown *hy5* mutants. In 30-d-old flowering plants, the expression of the *ProHY5-GUS* transgene was significantly reduced in leaves, stems, roots, and flowers of *hy5* and *cam7* mutants. The most drastic effect was observed in flowers, where the activity was reduced to ~5-fold in *hy5* mutants as compared with the wild type. Consistent with this observation, Hardtke et al. (2000) showed that HY5 accumulates at higher levels in flowers as compared with other organs during the inflorescence stage in adult plants. Collectively, this study demonstrates that HY5 and CAM7 act as positive regulators of *HY5* expression and highlights the transcriptional regulation of *HY5* in *Arabidopsis*.

METHODS

Plant Materials and Growth Conditions

The wild-type *Arabidopsis thaliana* and *cam7-1* and *hy5-215* null mutants used in this study are in the Col-0 background. The CAM7-GUS, cMyc-CAM7OE, cMyc-CAM7-M2OE, and cMyc-CAM3OE transgenic lines were generated as described by Kushwaha et al. (2008). Unless otherwise stated, seeds were surface-sterilized and plated on Murashige and Skoog medium supplemented with 0.8% Bactoagar (Difco) and 1% Suc. The plates were then cold treated at 4°C for 4 d and transferred to light chambers maintained at 22°C with the desired wavelength and intensity of light. For the growth of *Arabidopsis*, an LED chamber (Q-beam 3200-A; Quantum Devices) was used.

For the generation of *HY5 promoter-GUS* transgenic lines, the DNA fragment upstream of the start codon was PCR amplified and cloned into the pBI101.2 vector between restriction sites *Hin*dIII and *Xba*I. The *HY5 promoter*–driven *GUS* transgene was transferred into the wild type (Col-0) through *Agrobacterium tumefaciens*–mediated transformation by the vacuum infiltration method, and further lines carrying single-locus transgenes were identified and homozygous lines were generated as described by Hettiarachchi et al. (2003). The *ProHY5-GUS* transgene was then introduced into the *cam7-1* or *hy5-215* mutant background by genetic crosses with the wild-type transgenic lines as described by Yadav et al. (2002). The mutant lines homozygous for the transgene were obtained from the F3 generation for further studies. For the complementation test, a genomic fragment containing full-length *HY5* and the 0.5-kb upstream DNA sequence was amplified by PCR, cloned, and used for vacuum infiltration of *hy5* mutants containing the *ProHY5-GUS* transgene through *Agrobacterium* strain GV3101–mediated transformation.

Gel-Shift Assays and DNase I Footprinting

To determine the interaction between CAM7 or HY5 and the *HY5* promoter, a 127-bp DNA fragment of the *HY5* promoter containing the T/G- and E-boxes upstream of ATG (−330 to −204 bp) was cloned in pBluescript SK+, digested with *Xba*I-*Hin*dIII, purified, and 3′ end labeled with [α-^{32}P]dCTP (Chattopadhyay et al., 1998a). This fragment was used as a probe. The 85-bp fragment containing the T/G- and E-boxes was used for competition studies. The 85-bp DNA fragments of mutated T/G-box, mutated E-box, or mutated T/G- and E-boxes were designated as mT/G, mE, or mT/G&E, respectively. The various mutated versions of the 85-bp DNA fragment were constructed by primer-based site-directed mutagenesis. All these fragments were cloned into the pBluescript SK+ vector and subsequently digested with either *Hin*dIII-*Xba*I or *Xba*I-*Xho*I and purified for probe generation or competition assays. *Escherichia coli* purified GST-CAM7, GST-HY5, and GST were used for gel-shift or electrophoretic mobility-shift assays (Chattopadhyay et al., 1998a; Kushwaha et al., 2008).

Approximately 10 ng of labeled DNA fragment was incubated with purified protein in the presence of 1 μg of polydeoxyinosinic-polydeoxycytidylic acid and 1× binding buffer (5× = 75 mM HEPES, pH 7.6, 175 mM KCl, 10% glycerol, 5 mM DTT, and 1 mM $MgCl_2$) in a reaction volume of 30 μL for 20 to 25 min at room temperature. The reaction was terminated by DNA loading dye. Competition assays were performed using 50 and 100 molar excess of specific (wild-type) and nonspecific (mutated) fragments. The reactions were fractionated on a native polyacrylamide gel (12% acrylamide, 0.5× Tris-borate/EDTA, and 2.5% glycerol), dried, and autoradiographed. DNase I footprinting assays were performed essentially as described by Chattopadhyay et al. (1998a).

ChIP

The ChIP assays were performed essentially as described by Singh et al. (2012). Chromatin isolation was performed using 4-d-old seedlings of Col-0 and mutated or overexpresser transgenic seedlings grown under WL. The resuspended chromatin was sonicated at 4°C to ~0.5- to 1.0-kb fragments. The sheared chromatin was immunoprecipitated, washed, reverse cross-linked, and finally amplified (Kushwaha et al., 2008; Gangappa et al., 2010). About 10% of nonimmunoprecipitated sonicated chromatin was reverse cross-linked and used as an input DNA control. Both immunoprecipitated DNA and input DNA were analyzed by real-time PCR (Light Cycler; Roche). A polyclonal HY5 antibody (peptide-specific custom-made antibody generated by Sigma-Aldrich) or cMyc antibody (Sigma-Aldrich) was used for the assay.

GUS Assays

GUS staining and GUS activity measurements were performed by using 30 to 40 seedlings by following the procedure essentially as described previously (Chattopadhyay et al., 1998b; Mallappa et al., 2006; Bhatia et al., 2008). The wild type and *cam7-1* and *hy5-215* mutant transgenic lines containing the *ProHY5-GUS* transgene were stained for the same length of time.

In Vitro Binding and Pull-Down Assays

For in vitro binding assays, 2 μg of CAM7-6HIS or COP1-6HIS was individually bound to Ni-NTA beads. GST-HY5 or GST protein was added in an equimolar ratio. The beads and supernatant were collected separately by brief centrifugation, and beads were washed three times with 1 mL of wash buffer (50 mM Tris-HCl, pH 7.5, 100 mM NaCl, 10% glycerol, and 0.075% Tween 20). The pellet was resuspended in 1× SDS loading buffer, boiled for 10 min, and analyzed by SDS-PAGE. Both pellet and supernatant (5%) were analyzed by probing with anti-GST antibodies.

For in vitro pull-down experiments, GST and GST-HY5 proteins (1 μg each) were individually bound to GST beads. Approximately 1 mg of total protein extract from the CAM7-cMyc overexpression line was added and incubated at 4°C for 4 h. The beads and supernatant were collected separately by brief centrifugation, and beads were washed three times with 1 mL of wash buffer (50 mM Tris-HCl, pH 7.5, 100 mM NaCl, 10% glycerol, and 0.075% Tween 20). The pellet was resuspended in 1× SDS loading buffer, boiled for 10 min, and analyzed by SDS-PAGE. Both pellet and supernatant (5%) were analyzed by probing with anti-cMyc antibodies.

Colocalization and BiFC Assays

For colocalization studies, full-length HY5 was cloned in the pAM-PAT-35S-CFP vector to produce the HY5-CFP fusion protein, and similarly, CAM7 was cloned into the pAM-PAT-35S-YFP vector to produce the CAM7-YFP fusion protein (Datta et al., 2008). The colocalization experiment was performed using the same protocol as described by Singh et al. (2012).

For BiFC experiments, the full-length coding sequence of *CAM7* was cloned in the pUC-SPYNE vector to produce a fusion protein of CAM7-$YFP^{N\text{-}ter}$ and the full-length coding sequence of *HY5* was cloned in the pUC-SPYCE vector to obtain the HY5-$YFP^{C\text{-}ter}$ fusion. The BiFC experiments were performed in onion (*Allium cepa*) epidermal cells using a PDS-1000 Gene-gun (Bio-Rad), according to the method used for colocalization experiments. Empty vectors of BiFC constructs were used as a negative control. 4′,6-Diamidino-2-phenylindole staining was performed to identify the nuclei.

Gene Expression Analysis

Real-time PCR analyses were performed using the Thermal Cycler Applied Biosystem StepOne and Light Cycler Faststart DNA Masterplus SYBR Green 1 systems (Roche Applied Science). The transcript levels of *HY5* were determined, and the transcript levels were normalized with the level of *ACTIN2* transcript abundance.

Accession Numbers

Sequence data from this article can be found in the Arabidopsis Genome Initiative or GenBank/EMBL databases under the following accession numbers: *HY5*, AT5G11260; *CAM7*, AT3G43810; and *NIA2*, AT1G37130.

Supplemental Data

The following materials are available in the online version of this article.

Supplemental Figure 1. Various Transgenic Lines Containing the *ProHY5-GUS* Transgene.

Supplemental Figure 2. Activity of the *HY5* Promoter.

Supplemental Figure 3. CAM7, but Not CAM3, Promotes Photomorphogenic Growth.

Supplemental Figure 4. Expression of His Tag Proteins.

Supplemental Figure 5. DNase I Footprinting Analysis of the 127-bp *HY5* Promoter Region of the GST-HY5 or GST-CAM7 Protein.

Supplemental Table 1. Primer Sequences Used in This Study.

ACKNOWLEDGMENTS

We thank Hathi Ram (EMBL Heidelberg) for critically reading and commenting on the article. We thank Xing Wang Deng (Yale University) for providing us with the seeds of the HY5OE transgenic line. This work was supported by a J.C. Bose National Fellowship Award Grant from the Department of Science and Technology, Government of India, by a National Institute of Plant Genome Research internal grant to S.C., and by the following fellowships: from the Department of Biotechnology, Government of India, to N.A., from the Council of Scientific and Industrial Research, Government of India, to J.P.M., and from the National Institute of Technology to D.S.

AUTHOR CONTRIBUTIONS

N.A., J.P.M., and S.C. designed the research. N.A., J.P.M., D.S., and S.N.G. carried out the experiments. N.A., J.P.M., and S.C. analyzed the data and wrote the article.

Received December 31, 2013; revised December 31, 2013; accepted February 12, 2014; published March 7, 2014.

REFERENCES

Alabadí, D., Gallego-Bartolomé, J., Orlando, L., García-Cárcel, L., Rubio, V., Martínez, C., Frigerio, M., Iglesias-Pedraz, J.M., Espinosa, A., Deng, X.W., and Blázquez, M.A. (2008). Gibberellins modulate light signaling pathways to prevent Arabidopsis seedling de-etiolation in darkness. Plant J. **53:** 324–335.

Anderson, S.L., Teakle, G.R., Martino-Catt, S.J., and Kay, S.A. (1994). Circadian clock- and phytochrome-regulated transcription is conferred by a 78 bp cis-acting domain of the Arabidopsis CAB2 promoter. Plant J. **6:** 457–470.

Andronis, C., Barak, S., Knowles, S.M., Sugano, S., and Tobin, E.M. (2008). The clock protein CCA1 and the bZIP transcription factor HY5 physically interact to regulate gene expression in Arabidopsis. Mol. Plant **1:** 58–67.

Ang, L.H., and Deng, X.W. (1994). Regulatory hierarchy of photomorphogenic loci: Allele-specific and light-dependent interaction between the HY5 and COP1 loci. Plant Cell **6:** 613–628.

Ang, L.H., Chattopadhyay, S., Wei, N., Oyama, T., Okada, K., Batschauer, A., and Deng, X.W. (1998). Molecular interaction between COP1 and HY5 defines a regulatory switch for light control of Arabidopsis development. Mol. Cell **1:** 213–222.

Arguello-Astorga, G., and Herrera-Estrella, L. (1998). Evolution of light-regulated plant promoters. Annu. Rev. Plant Physiol. Plant Mol. Biol. **49:** 525–555.

Bhatia, S., Gangappa, S.N., Kushwaha, R., Kundu, S., and Chattopadhyay, S. (2008). SHORT HYPOCOTYL IN WHITE LIGHT1, a serine-arginine-aspartate-rich protein in Arabidopsis, acts as a negative regulator of photomorphogenic growth. Plant Physiol. **147:** 169–178.

Bhattacharya, S., Bunick, C.G., and Chazin, W.J. (2004). Target selectivity in EF-hand calcium binding proteins. Biochim. Biophys. Acta **1742:** 69–79.

Cashmore, A.R., Jarillo, J.A., Wu, Y.J., and Liu, D. (1999). Cryptochromes: Blue light receptors for plants and animals. Science **284:** 760–765.

Chang, C.S., Li, Y.H., Chen, L.T., Chen, W.C., Hsieh, W.P., Shin, J., Jane, W.N., Chou, S.J., Choi, G., Hu, J.M., Somerville, S., and Wu, S.H. (2008). LZF1, a HY5-regulated transcriptional factor, functions in Arabidopsis de-etiolation. Plant J. **54:** 205–219.

Chattopadhyay, S., Ang, L.H., Puente, P., Deng, X.W., and Wei, N. (1998a). *Arabidopsis* bZIP protein HY5 directly interacts with light-responsive promoters in mediating light control of gene expression. Plant Cell **10:** 673–683.

Chattopadhyay, S., Puente, P., Deng, X.W., and Wei, N. (1998b). Combinatorial interaction of light-responsive elements plays a critical role in determining the response characteristics of light-regulated promoters in Arabidopsis. Plant J. **15:** 69–77.

Chen, H., Zhang, J., Neff, M.M., Hong, S.W., Zhang, H., Deng, X.W., and Xiong, L. (2008). Integration of light and abscisic acid signaling during seed germination and early seedling development. Proc. Natl. Acad. Sci. USA **105:** 4495–4500.

Chen, M., Chory, J., and Fankhauser, C. (2004). Light signal transduction in higher plants. Annu. Rev. Genet. **38:** 87–117.

Cluis, C.P., Mouchel, C.F., and Hardtke, C.S. (2004). The Arabidopsis transcription factor HY5 integrates light and hormone signaling pathways. Plant J. **38:** 332–347.

Datta, S., Johansson, H., Hettiarachchi, C., Irigoyen, M.L., Desai, M., Rubio, V., and Holm, M. (2008). LZF1/SALT TOLERANCE HOMOLOG3, an *Arabidopsis* B-box protein involved in light-dependent development and gene expression, undergoes COP1-mediated ubiquitination. Plant Cell **20:** 2324–2338.

Degenhardt, J., and Tobin, E.M. (1996). A DNA binding activity for one of two closely defined phytochrome regulatory elements in an Lhcb promoter is more abundant in etiolated than in green plants. Plant Cell **8:** 31–41.

Feldbrügge, M., Sprenger, M., Hahlbrock, K., and Weisshaar, B. (1997). PcMYB1, a novel plant protein containing a DNA-binding domain with one MYB repeat, interacts in vivo with a light-regulatory promoter unit. Plant J. **11:** 1079–1093.

Gangappa, S.N., Prasad, V.B., and Chattopadhyay, S. (2010). Functional interconnection of MYC2 and SPA1 in the photomorphogenic seedling development of Arabidopsis. Plant Physiol. **154:** 1210–1219.

Gilmartin, P.M., Sarokin, L., Memelink, J., and Chua, N.H. (1990). Molecular light switches for plant genes. Plant Cell **2:** 369–378.

Grabarek, Z. (2006). Structural basis for diversity of the EF-hand calcium-binding proteins. J. Mol. Biol. **359:** 509–525.

Hardtke, C.S., Gohda, K., Osterlund, M.T., Oyama, T., Okada, K., and Deng, X.W. (2000). HY5 stability and activity in Arabidopsis is regulated by phosphorylation in its COP1 binding domain. EMBO J. **19:** 4997–5006.

Hashimoto, K., and Kudla, J. (2011). Calcium decoding mechanisms in plants. Biochimie **93:** 2054–2059.

Hettiarachchi, G.H.C.M., Yadav, V., Reddy, M.K., Chattopadhyay, S., and Sopory, S.K. (2003). Light-mediated regulation defines a minimal promoter region of TOP2. Nucleic Acids Res. **31:** 5256–5265.

Holm, M., Ma, L.G., Qu, L.J., and Deng, X.W. (2002). Two interacting bZIP proteins are direct targets of COP1-mediated control of light-dependent gene expression in *Arabidopsis*. Genes Dev. **16:** 1247–1259.

Ikura, M., Osawa, M., and Ames, J.B. (2002). The role of calcium-binding proteins in the control of transcription: Structure to function. Bioessays **24:** 625–636.

Jiao, Y., Lau, O.S., and Deng, X.W. (2007). Light-regulated transcriptional networks in higher plants. Nat. Rev. Genet. **8:** 217–230.

Kehoe, K.M., Degenhardt, J., Winicov, I., and Tobin, E.M. (1994). Photomorphogenesis in Plants, 2nd ed. (Dordrecht, The Netherlands: Martinus Nijhoff/Dr. W. Junk).

Koornneef, M., Rolff, E., and Spruit, C.J.P. (1980). Genetic control of light inhibited hypocotyl elongation in Arabidopsis thaliana. Z. Pflanzenphysiol. **100:** 147–160.

Kushwaha, R., Singh, A., and Chattopadhyay, S. (2008). Calmodulin7 plays an important role as transcriptional regulator in *Arabidopsis* seedling development. Plant Cell **20:** 1747–1759.

Lee, J., He, K., Stolc, V., Lee, H., Figueroa, P., Gao, Y., Tongprasit, W., Zhao, H., Lee, I., and Deng, X.W. (2007). Analysis of transcription factor HY5 genomic binding sites revealed its hierarchical role in light regulation of development. Plant Cell **19:** 731–749.

Li, J., Li, G., Gao, S., Martinez, C., He, G., Zhou, Z., Huang, X., Lee, J.H., Zhang, H., Shen, Y., Wang, H., and Deng, X.W. (2010). *Arabidopsis* transcription factor ELONGATED HYPOCOTYL5 plays a role in the feedback regulation of phytochrome A signaling. Plant Cell **22:** 3634–3649.

Lin, C. (2002). Blue light photoreceptors and signal transduction. Plant Cell **14**(suppl.)**:** S207–S225.

Luan, S., Kudla, J., Rodriguez-Concepcion, M., Yalovsky, S., and Gruissem, W. (2002). Calmodulins and calcineurin B-like proteins: Calcium sensors for specific signal response coupling in plants. Plant Cell **14** (suppl.)**:** S389–S400.

Ma, L., Li, J., Qu, L., Hager, J., Chen, Z., Zhao, H., and Deng, X.W. (2001). Light control of *Arabidopsis* development entails coordinated regulation of genome expression and cellular pathways. Plant Cell **13:** 2589–2607.

Mallappa, C., Singh, A., Ram, H., and Chattopadhyay, S. (2008). GBF1, a transcription factor of blue light signaling in Arabidopsis, is degraded in the dark by a proteasome-mediated pathway independent of COP1 and SPA1. J. Biol. Chem. **283:** 35772–35782.

Mallappa, C., Yadav, V., Negi, P., and Chattopadhyay, S. (2006). A basic leucine zipper transcription factor, G-box-binding factor 1, regulates blue light-mediated photomorphogenic growth in Arabidopsis. J. Biol. Chem. **281:** 22190–22199.

Manzara, T., Carrasco, P., and Gruissem, W. (1991). Developmental and organ-specific changes in promoter DNA-protein interactions in the tomato *rbcS* gene family. Plant Cell **3:** 1305–1316.

McCormack, E., Tsai, Y., and Braam, J. (2005). Handling calcium signalling: *Arabidopsis* CaMs and CMLs. Trends Plant Sci. **10:** 383–389.

McNellis, T.W., and Deng, X.W. (1995). Light control of seedling morphogenetic pattern. Plant Cell **7:** 1749–1761.

Nagatani, A., Chory, J., and Furuya, M. (1993). Phytochrome B is not detectable in the hy3 mutant of Arabidopsis, which is deficient in responding to end-of-day far-red-light treatments. Plant Cell Physiol. **32:** 1119–1122.

Neff, M.M., Fankhauser, C., and Chory, J. (2000). Light: An indicator of time and place. Genes Dev. **14:** 257–271.

Osawa, M., Dace, A., Tong, K.I., Valiveti, A., Ikura, M., and Ames, J.B. (2005). Mg^{2+} and Ca^{2+} differentially regulate DNA binding and dimerization of DREAM. J. Biol. Chem. **280:** 18008–18014.

Osterlund, M.T., Hardtke, C.S., Wei, N., and Deng, X.W. (2000). Targeted destabilization of HY5 during light-regulated development of Arabidopsis. Nature **405:** 462–466.

Oyama, T., Shimura, Y., and Okada, K. (1997). The Arabidopsis HY5 gene encodes a bZIP protein that regulates stimulus-induced development of root and hypocotyl. Genes Dev. **11:** 2983–2995.

Pepper, A.E., and Chory, J. (1997). Extragenic suppressors of the Arabidopsis det1 mutant identify elements of flowering-time and light-response regulatory pathways. Genetics **145:** 1125–1137.

Perochon, A., Aldon, D., Galaud, J.P., and Ranty, B. (2011). Calmodulin and calmodulin-like proteins in plant calcium signaling. Biochimie **93:** 2048–2053.

Reddy, A.S. (2001). Calcium: Silver bullet in signaling. Plant Sci. **160:** 381–404.

Rohde, A., Van Montagu, M., and Boerjan, W. (1999). The ABSCISIC ACID INSENSITIVE 3 (ABI3) gene is expressed during vegetative quiescence processes in Arabidopsis. Plant Cell Environ. **22:** 261–270.

Schepens, I., Duek, P., and Fankhauser, C. (2004). Phytochrome-mediated light signalling in Arabidopsis. Curr. Opin. Plant Biol. **7:** 564–569.

Shin, J., Park, E., and Choi, G. (2007). PIF3 regulates anthocyanin biosynthesis in an HY5-dependent manner with both factors directly binding anthocyanin biosynthetic gene promoters in Arabidopsis. Plant J. **49:** 981–994.

Sibout, R., Sukumar, P., Hettiarachchi, C., Holm, M., Muday, G.K., and Hardtke, C.S. (2006). Opposite root growth phenotypes of *hy5* versus *hy5 hyh* mutants correlate with increased constitutive auxin signaling. PLoS Genet. **2:** e202.

Singh, A., Ram, H., Abbas, N., and Chattopadhyay, S. (2012). Molecular interactions of GBF1 with HY5 and HYH proteins during light-mediated seedling development in *Arabidopsis thaliana*. J. Biol. Chem. **287:** 25995–26009.

Snedden, W.A., and Fromm, H. (2001). Calmodulin as a versatile calcium signal transducer in plants. New Phytol. **151:** 35–66.

Song, Y.H., et al. (2008). DNA-binding study identifies C-box and hybrid C/G-box or C/A-box motifs as high-affinity binding sites for STF1 and LONG HYPOCOTYL5 proteins. Plant Physiol. **146:** 1862–1877.

Tepperman, J.M., Zhu, T., Chang, H.S., Wang, X., and Quail, P.H. (2001). Multiple transcription-factor genes are early targets of phytochrome A signalling. Proc. Natl. Acad. Sci. USA **98:** 9437–9442.

Terzaghi, W.B., and Cashmore, A.R. (1995). Light-regulated transcription. Annu. Rev. Plant Physiol. Plant Mol. Biol. **46:** 445–474.

Tobin, E.M., and Kehoe, D.M. (1994). Phytochrome regulated gene expression. Semin. Cell Biol. **5:** 335–346.

Vandenbussche, F., Habricot, Y., Condiff, A.S., Maldiney, R., Van der Straeten, D., and Ahmad, M. (2007). HY5 is a point of convergence between cryptochrome and cytokinin signalling pathways in *Arabidopsis thaliana*. Plant J. **49:** 428–441.

Whitelam, G.C., Johnson, E., Peng, J., Carol, P., Anderson, M.L., Cowl, J.S., and Harberd, N.P. (1993). Phytochrome A null mutants of *Arabidopsis* display a wild-type phenotype in white light. Plant Cell **5:** 757–768.

Yadav, V., Kundu, S., Chattopadhyay, D., Negi, P., Wei, N., Deng, X. W., and Chattopadhyay, S. (2002). Light regulated modulation of Z-box containing promoters by photoreceptors and downstream regulatory components, COP1 and HY5, in Arabidopsis. Plant J. **31:** 741–753.

Yadav, V., Mallappa, C., Gangappa, S.N., Bhatia, S., and Chattopadhyay, S. (2005). A basic helix-loop-helix transcription factor in *Arabidopsis*, MYC2, acts as a repressor of blue light-mediated photomorphogenic growth. Plant Cell **17:** 1953–1966.

Yang, T., and Poovaiah, B.W. (2003). Calcium/calmodulin-mediated signal network in plants. Trends Plant Sci. **8:** 505–512.

Zielinski, R.E. (1998). Calmodulin and calmodulin-binding proteins in plants. Annu. Rev. Plant Physiol. Plant Mol. Biol. **49:** 697–725.